

## EXPERIENCE OF TRIPLE-SOURCE AIRGUN ARRAY PERFORMANCE.

Jonathan Pollatos, Stuart Denny, Sergio Grion, Rob Telling, R. Gareth Williams (Shearwater GeoServices)

**Introduction:** Triple-source, and in general multi-source streamer acquisitions have gained increasing interest and application during the last 3 years in the wake of proposals in [1] and [2]. This type of surveys introduces a more flexible arrangement of sources and cables that can lead to efficiency and resolution gains.

For conventional dual-source flip-flop acquisitions the source arrays are closer to each other and symmetrically placed with respect to the boat, and therefore exhibit similar performance behaviour. For a triple or multi-source array however, the wider spacing (75m from port to starboard source centres instead of 50m for typical dual source recording) may introduce changes in source array performance due to different positions of the arrays with respect to the ship's wake. In this paper, we use navigation and near-field-hydrophone data to characterize and explain differences in performance between the port, central and starboard sources of triple-source acquisitions carried out in the Barents Sea and Atlantic Margin in 2017. In particular, we investigate small but consistent variations in performance between the central source and the outer sources, and whether it is differences in tow stability or differences in sea-surface state above the sources that is causing these performance variations.

### Triple source acquisition

During the Northern Hemisphere summer months, Shearwater GeoServices acquired approximately 26,000 sq. km of triple source data on behalf of TGS. The data was recorded using three vessels working on three different projects in the Barents sea and the Atlantic margin of Norway and Ireland. Figure 1 shows the towing configuration with three dual string arrays towed with a separation of 37.5m between each array centre. The configuration was the same on each of the vessels. This recording geometry provides 18.75m crossline CMP bin size, with no interpo-

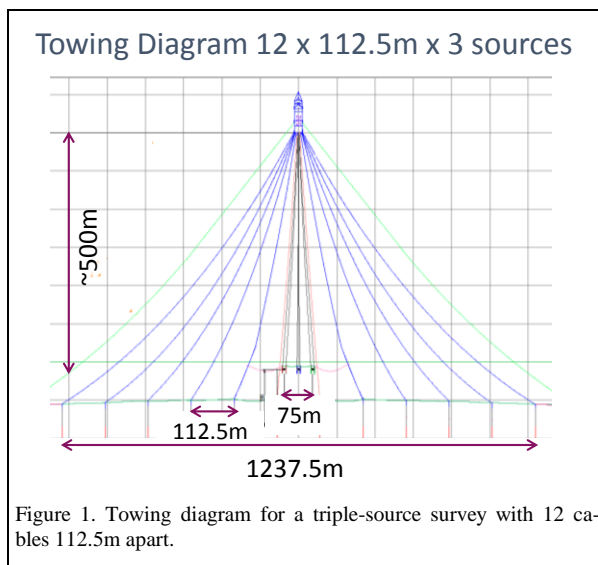


Figure 1. Towing diagram for a triple-source survey with 12 cables 112.5m apart.

lation applied, even with a wider than normal streamer spacing of 112.5m.

The source arrays are towed approximately 500m behind the stern of the vessel. As described above, one consequence of this triple source arrangement is that the central source will, in general, lie within the wake of the vessel. Therefore a number of questions arise about the performance of the central array compared to the outer arrays. Will the turbulence from the vessel propulsion cause greater technical downtime than normal and will the source stability be reduced by the turbulence? Or does the flatter sea surface provide a more stable source signature and source ghost?

**Source technical down time:** Triple source acquisition with two strings per array required a modified array design and also a modified towing configuration compared to the conventional three string, dual source arrangement. Despite these changes, the technical downtime associated with sources and towing of sources was still approximately 1/3<sup>rd</sup> of the total technical downtime. Given the typical weather conditions in the Atlantic Margin and Barents Sea this compares favourably with statistics averaged over the whole of a previous year in a wide variety of environments.

**On board quality control of airgun signatures:** As part of the routine onboard QC procedures, the far field signature is computed from the recorded near field hydrophones on a shot by shot basis. These far fields are plotted and examined by the onboard processors but they are also cross-correlated against a reference signature. This allows quick identification of any variability or changes in the source signature.

The reference far field signature is obtained by computing the far field over a number of shots before the start of a survey and then averaging these individual signatures. In the case of triple source, each array is fired a number of times and the average is computed across all three arrays. Thus, there should be no bias when cross-correlating an individual source to this average reference signature.

Figure 2 shows the shot-by-shot cross-correlation for all three sources for one line 45km long. All three sources are well correlated to the reference, with cross-correlation values always above 0.994. However inspection of Figure 2 clearly shows that the port and starboard sources have

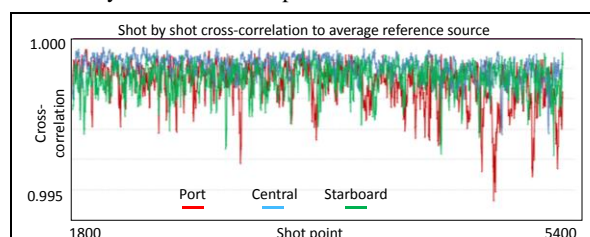


Figure 2. On board signatures QC showing higher cross-correlation values for the central source.

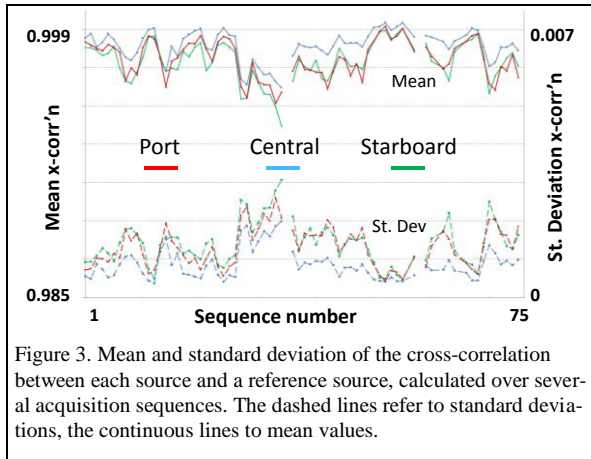


Figure 3. Mean and standard deviation of the cross-correlation between each source and a reference source, calculated over several acquisition sequences. The dashed lines refer to standard deviations, the continuous lines to mean values.

greater variability than the central array and also have occasional outliers.

Figure 3 shows the mean cross-correlation for each array averaged over a shot line and plotted for 75 sequences within one particular survey. It can be seen that the central array consistently has a higher average cross-correlation across the project. Figure 3 also shows the standard deviation of each source array for each sequence within the survey. This shows that the variability of the central source along each sequence is also consistently low. Whilst a systematic bias in the reference source towards the central source could explain the consistently higher cross-correlation, it would not explain the decreased variability of the central source. Furthermore, similar results have been found on more than one vessel suggesting a geophysical reason for this behaviour

Both these QC plots (Figure 1 and Figure 2) indicate that the central array is more stable than the outer sources in its output. Two possible factors that could be causing this are a) the string separation within each array is more stable in the wake of the vessel or b) the rough sea surface has been smoothed out by the vessel wake and hence a more stable source ghost is produced.

**Source positioning analysis:** A possible cause of differing performance for the three arrays is the positioning of the array strings relative to each other. To investigate if positioning plays a role in determining the cross-correlation values in Figure 2 and Figure 3, we analysed string locations using GPS positions for the head and tail of each string, for a number of adjacent shots. Figure 4 shows the location of each string relative to the midpoint of each array. The string locations show a high degree of overlap for these shots, as shown in Figure 4. Numerical averages of string distances are 7.63 for the starboard source, 7.48m for the central source and 7.15m for the port source, thus showing that distances have very similar values for the three arrays and that for the central array positioning is closest to the nominal 7.5m separation value. The standard deviations related to these averages are 8.5cm for the starboard source, 13.5cm for the central source and 12cm for the port source. While the central source is closest to nominal separation on average, its standard deviation is not the lowest. This observation,

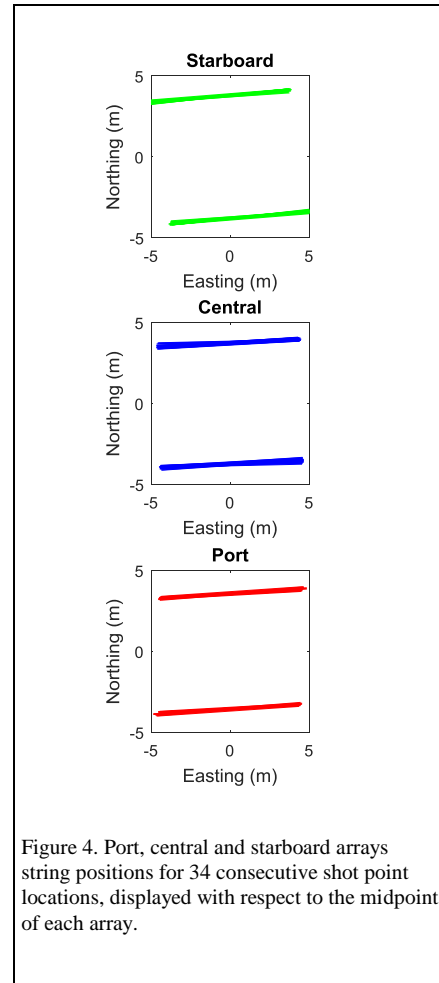


Figure 4. Port, central and starboard arrays string positions for 34 consecutive shot point locations, displayed with respect to the midpoint of each array.

together with the overall small deviations from nominal of all three sources, suggests that positioning may not be the main cause of the observed higher average correlation and lower standard deviation observed in the QC plots in Figure 2 and 3.

**Near-field hydrophones data inversion:** In past work [3] we have described a method for deriving directional far-field signatures from near-gun recordings. In this section, we recall and summarize this work, based on a form of least-squares inversion. In our method, as in [4], we use data from hydrophones placed close to each gun in the array to obtain estimates of the “notional signature” of each gun, which is the signature obtained when the gun is firing in the pressure field generated by the other guns. Once notional signatures have been derived for a particular shot they can be used to construct far-field signatures at any desired direction away from the array.

Our method is an alternative to the commonly used iterative approach proposed by [5]. Its main advantage is that it is more accurate at low frequencies, since it correctly handles the motion of the air bubble as it moves away from the gun and towards other hydrophones. This is a problematic aspect of the iterative approach, which can cause low frequency inaccuracies, and in some circumstances instability in the solution.

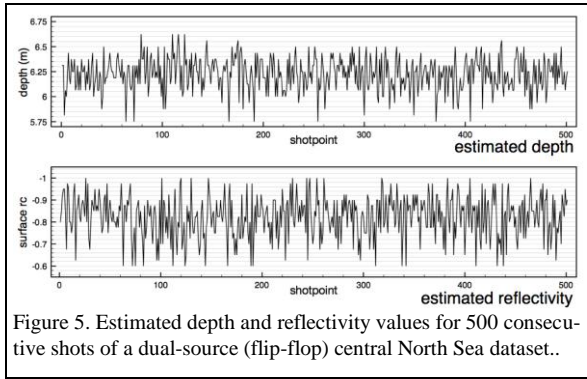


Figure 5. Estimated depth and reflectivity values for 500 consecutive shots of a dual-source (flip-flop) central North Sea dataset..

A complication in both approaches is the need to model and remove the sea-surface ghost from the near-gun records. The notional signatures are by definition unghosted, but the records for each hydrophone contain contributions both from energy that has travelled directly to the hydrophone and also from energy that has travelled by reflection from the sea-surface. Accurate derivation of the notional signatures requires knowledge of the characteristics of the ghost – in the simplest case, the depth of the array and an average frequency-dependent sea-surface reflection coefficient.

We derive shot-by-shot estimates of the array depth and sea-surface reflectivity as part of the signature estimation. Our method follows from the somewhat unexpected observation that the near-field data can contain a strong ghost component, such that there is a noticeable sensitivity of derived signatures to the depth and reflectivity parameters used for their computation [6]. The form we assume for describing sea-surface reflectivity as a function of wave height follows the coherent scattering analysis in [7]. Furthermore, equating Gaussian roughness to one quarter of the significant wave height SWH gives, for vertical incidence, the reflectivity  $R = \exp(-0.5(\pi f SWH/v)^2)$ , where  $f$  is frequency in Hz and  $v$  is the sound speed in water (m/s) in the vicinity of the source. The optimization for array depth and wave height finds the combination of parameters that yield the minimum residual with respect to a linear least squares trend in the summed notional spectra, in a targeted frequency band around the ghost notch.

As an example, Figure 5 shows estimated depth and 100Hz sea-surface reflectivity for 500 consecutive shots of

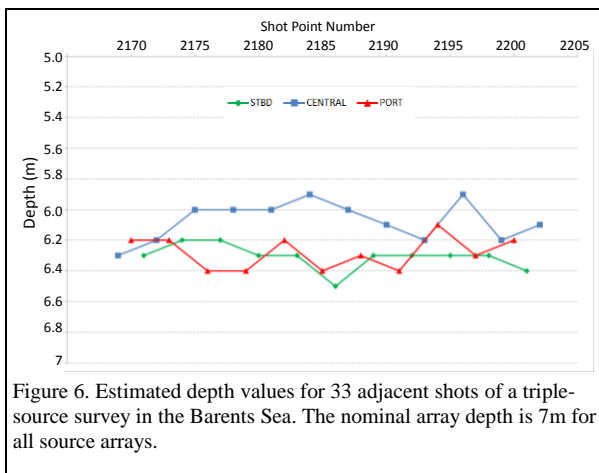


Figure 6. Estimated depth values for 33 adjacent shots of a triple-source survey in the Barents Sea. The nominal array depth is 7m for all source arrays.

a central North sea dataset, as published in [6]. Variations in depths are associated with average water-column height changes from shot to shot which influence the source ghost period. The estimated 100 Hz reflectivities can be related to a significant wave-height (SWH) during acquisition, and determines the average frequency-dependent sea-surface reflectivity.

**Sea surface reflectivities and array depths:** Figures 6 and 7 show the estimated source array depths and significant wave-height estimated from near-field hydrophone data for the Barents Sea triple-source survey. The estimated depths are shallower than the nominal value of 7m, and slightly shallower for the central source with respect to port and starboard. The SWH for the central source is zero for all the examined source locations, while port and starboard values are higher and more variable, thus showing that the sea-surface above the central source is calmer.

Figure 8 shows the estimated vertical far-field signatures for the three arrays, without optimization. The source ghost is not included in the far-field calculation but it present in the near-field hydrophone data. The inversion process that calculates the notional signatures removes the effect of the source ghost, that can then be optionally applied in the calculation of the far field signatures. A typical feature of non-optimised signatures is the oscillations visible close to the main pulse, which occur at the source ghost notch frequency. These occur when the source ghost model used for NFH inversion is not accurate. When the optimised parameters of figures 6 and 7 are used, the obtained signatures in Figure 9 are free from these oscillations. This demonstrates that the optimised parameters provide a better description of the source ghost than the nominal parameters used to calculate the signatures in Figure 8 (7m array depths and 1.5m SWH).

Inspection of Figures 8 and 9 also shows that the main pulse for the three arrays is stable and spatially consistent. The bubble oscillations however are more variable. It is therefore anticipated that the use of NFH data will benefit signature deconvolution.

**Conclusions:** There are three conclusions we can draw from our observations of acquisition technical downtime, QC displays, array positioning and estimated array depths and sea-surface reflectivities. First, positioning a source

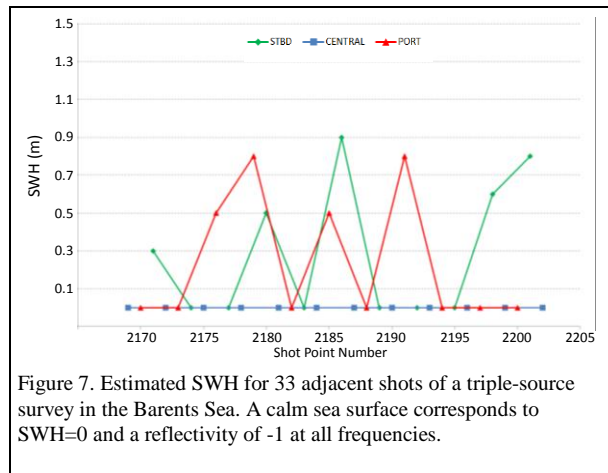


Figure 7. Estimated SWH for 33 adjacent shots of a triple-source survey in the Barents Sea. A calm sea surface corresponds to SWH=0 and a reflectivity of -1 at all frequencies.

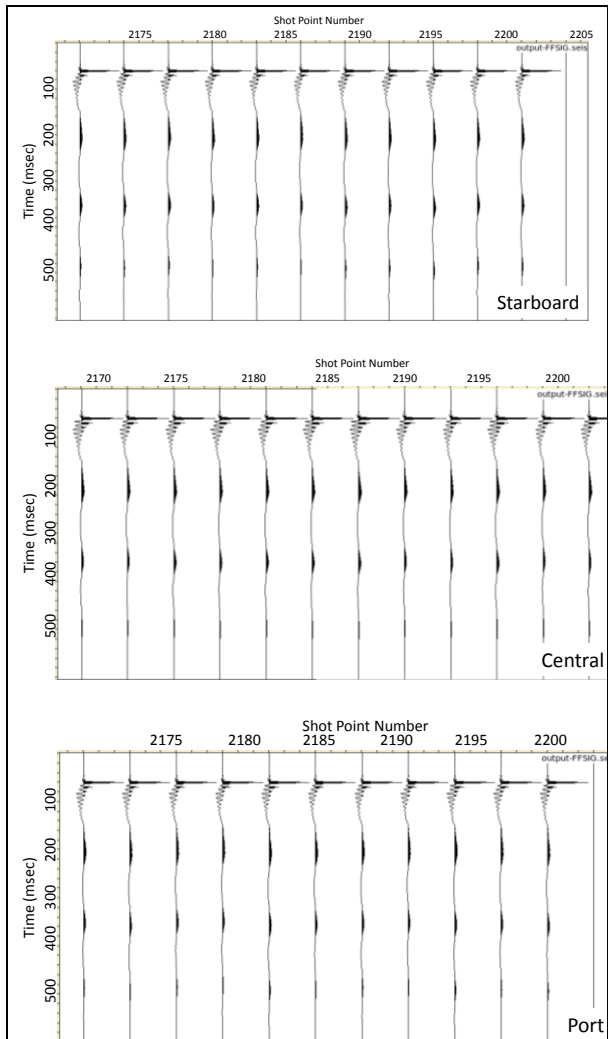


Figure 8 Estimated vertical far-field signatures for starboard, central and port source arrays, without optimization.

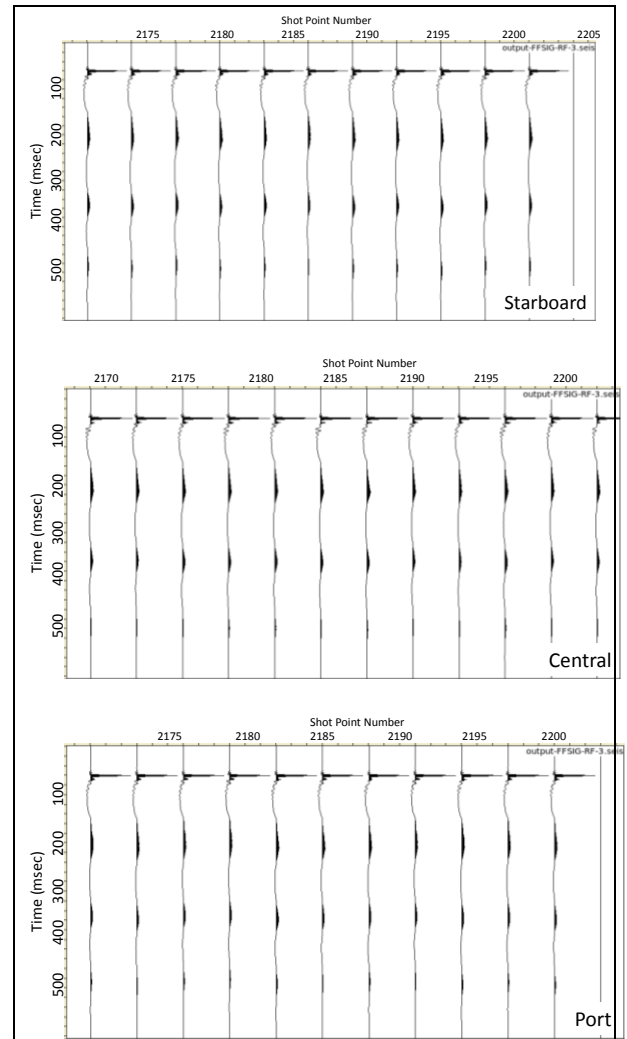


Figure 9 Estimated vertical far-field signatures for starboard, central and port source arrays, with optimization.

array within the wake of the vessel does not lead to more technical downtime that counteracts the efficiency gains of triple source and wider cable spacing. Second, the central source is a little more stable than the port and starboard arrays but all sources perform adequately, thus ensuring that the data quality gains from smaller crossline bin sizes are not compromised by a more variable source signature propagating in to the earth. Third, the improved stability of the central source does not appear to be related to string separation but may be related to a smoother sea surface within the wake of the vessel. Further data will be analysed to test whether this conclusion is confirmed

**Acknowledgements:** The authors would like to thank TGS for permission to show the near-field hydrophone data and on-board QC displays from the Barents Sea survey carried out by Shearwater in 2017.

**References:** [1] Langhammer, J., Bennion, P. (2015) Triple-source simultaneous shooting (TS3), a future for higher density seismic?, EAGE 2015 Extended Abstracts, We N101 06. [2] Hager, E., Rocke, M., Fontana, P. (2015) Efficient multi-source and multi-streamer configuration for dense cross-line sampling, SEG 2015 Expanded Abstracts,

100-104. [3] Hargreaves N., Grion S. and Telling, R. (2015) Estimation of air-gun array signatures from near-gun measurements - least-squares inversion, bubble motion and error analysis, SEG 2015 Expanded Abstracts, 149-153. [4] Ziolkowski, A., Parkes, G.E, Hatton L and Haugland T. (1982) The signature of an air gun array: computation from near-field measurements including interactions: *Geophysics*, 47, 1413-1421. [5] Parkes G.E., A. Ziolkowski A., L. Hatton L. and Haugland T. (1984), The signature of an airgun array: computation from near-field measurements including interactions – practical considerations: *Geophysics*, 49, 105–111.[6] Hargreaves, N., Telling, R., Grion, S. (2016) Source de-ghosting and directional designature using near-field derived airgun signatures, EAGE 2016 Expanded Abstracts, We SRS3 16. [7] Medwin H. and Clay C. S. (1998), *Fundamentals of Acoustical Oceanography*, Academic Press.